



Research Article

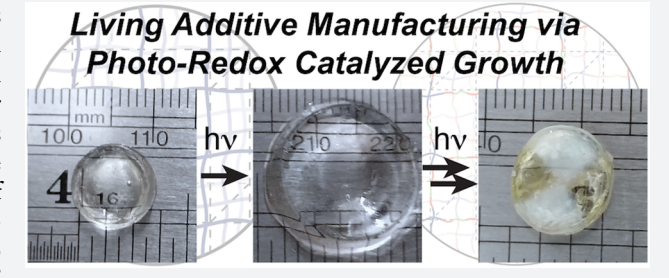
http://pubs.acs.org/journal/acscii

Living Additive Manufacturing: Transformation of Parent Gels into Diversely Functionalized Daughter Gels Made Possible by Visible **Light Photoredox Catalysis**

Mao Chen, $^{\dagger,\#,\perp}$ Yuwei Gu, $^{\dagger,\#}$ Awaneesh Singh, ‡ Mingjiang Zhong, $^{\dagger,\$,\P_{\textcircled{\scriptsize 0}}}$ Alex M. Jordan, $^{\parallel}$ Santidan Biswas, ‡ LaShanda T. J. Korley, $^{\parallel_{\textcircled{\scriptsize 0}}}$ Anna C. Balazs, ‡ and Jeremiah A. Johnson*, $^{\dagger_{\textcircled{\scriptsize 0}}}$

Supporting Information

ABSTRACT: Light-initiated additive manufacturing techniques typically rely on layer-by-layer addition or continuous extraction of polymers formed via nonliving, free radical polymerization methods that render the final materials "dead" toward further monomer insertion; the polymer chains within the materials cannot be reactivated to induce chain extension. An alternative "living additive manufacturing" strategy would involve the use of photocontrolled living radical polymerization to spatiotemporally insert monomers into dormant "parent" materials to generate more complex and diversely functionalized "daughter"



materials. Here, we demonstrate a proof-of-concept study of living additive manufacturing using end-linked polymer gels embedded with trithiocarbonate iniferters that can be activated by photoinduced single-electron transfer from an organic photoredox catalyst in solution. This system enables the synthesis of a wide range of chemically and mechanically differentiated daughter gels from a single type of parent gel via light-controlled modification of the parent's average composition, strand length, and/or cross-linking density. Daughter gels that are softer than their parent, stiffer than their parent, larger but with the same modulus as their parent, thermally responsive, polarity responsive, healable, and weldable are all realized.

7ith nearly 40 years of extensive development, photoinitiated free radical polymerization is unequivocally a robust and versatile technique for material fabrication with numerous applications in coatings, adhesives, microelectronics, optics, and biomaterials. In particular, new three-dimensional (3D) printing systems that leverage the speed and oxygen sensitivity of free radical polymerization have enabled remarkable advances in additive manufacturing.^{2,3} Despite these demonstrated successes, the chemistry of free radical polymerization has limitations that preclude certain potentially desirable features of 3D printed objects. Most notably, polymers produced via free radical processes cannot be reinitiated to induce chain extension (Figure 1a); these polymers are not "living". Thus, in the context of additive manufacturing, materials made via layer-by-layer or continuous solid-liquid interface methods that use traditional free radical polymerization cannot be subsequently reactivated after fabrication to introduce new monomers and/or functionality in a living fashion.

An alternative living additive manufacturing approach could involve the spatiotemporal insertion of monomers and/or cross-linkers directly into the strands of an existing polymeric network to convert the "parent" network into a new "daughter"

network with altered shape, composition, and properties (Figure 1b). To realize living additive manufacturing, a highly controlled, light-regulated⁵⁻⁹ living polymerization capable of repeated insertion of monomers into dynamic covalent polymer networks without side reactions or significant termination is needed. Though there are many examples where light is used to alter the composition, structure, shape, motion, dynamics, and mechanics of polymer networks, 10-21 often using sulfur-based functional groups as dynamic covalent bonds, 22-30 none have been proven capable of living insertion of new monomers to achieve additive growth of the material as described in Figure

To our knowledge, there are only two reports wherein photoinduced insertion of monomers into polymer network strands is investigated experimentally; 31,32 neither involves living chain growth (note: we have also investigated such processes using simulations that neglect termination reactions and thereby model a living polymerization³³). In 2013, we reported the photoinduced insertion of N-isopropylacrylamide (NIPAAM) into the strands of polymer networks using an

Received: November 7, 2016 Published: January 13, 2017



[†]Department of Chemistry and [§]Department of Chemical Engineering, Massachusetts Institute of Technology, 77 Massachusetts Avenue, Cambridge, Massachusetts 02139, United States

[‡]Chemical Engineering Department, University of Pittsburgh, Pittsburgh, Pennsylvania 15261, United States

Department of Macromolecular Science and Engineering, Case Western Reserve University, Cleveland, Ohio 44106, United States

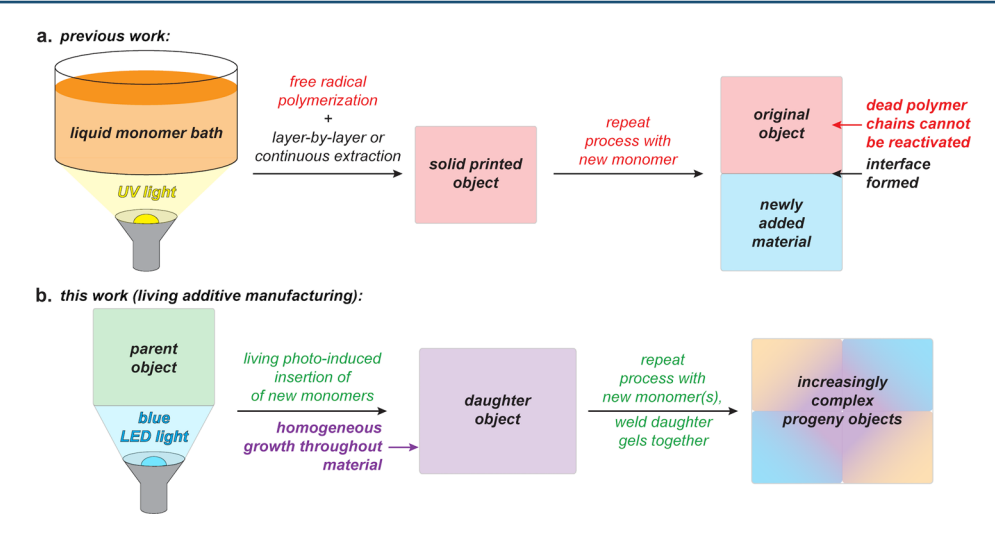


Figure 1. Comparison of traditional light-induced additive manufacturing and proposed living additive manufacturing. (a) Free radical polymerization produces materials with chains that cannot be reactivated for insertion of new monomers. Though extremely well developed, these methods cannot achieve homogeneous modification of already printed objects. (b) Herein, we develop a living additive manufacturing approach wherein parent objects comprised of dynamic covalent polymer networks are reactivated via a photoinduced living radical polymerization to generate daughter objects with homogeneous network modifications. These daughter objects of varying composition can be welded together to form increasingly complex progeny with spatially defined stimuli-responsive behaviors.

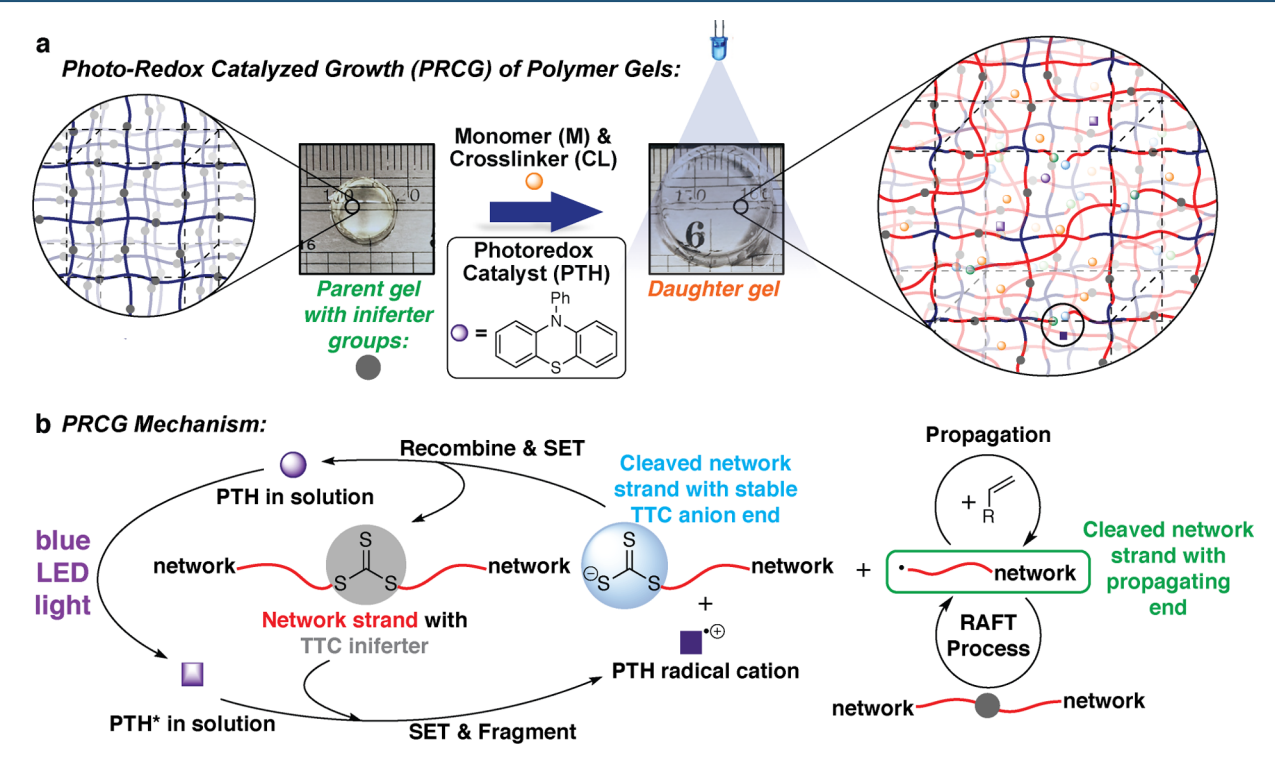


Figure 2. Photoredox catalyzed growth (PRCG) of cross-linked polymer gels. (a) General schematic for controlling polymer network structure by PRCG. Monomers (M) and cross-linkers (CL) can be directly incorporated into the network strands via a living photoredox catalyzed process. (b) Proposed mechanism of PRCG polymerization using a suitable photocatalyst (10-phenylphenothiazine, PTH) and a network comprised of strands bearing trithiocarbonate (TTC) iniferters. Blue LED light excites PTH molecules in solution and leads to photoinduced electron transfer from PTH* to the network-bound TTCs. Strand cleavage produces a propagating strand (green), a strand with a stable TTC anion (blue), and the PTH radical cation in solution (purple). In the presence of monomers (M) or cross-linkers (CL), the propagating strand can grow; it can also undergo degenerative chain transfer ("RAFT process") with adjacent nonactivated network strands. Turning the light source "OFF" leads to recombination of the cleaved strands via back electron transfer to the PTH radical cation, thereby resulting in net photocontrolled insertion of new M and CL into the network in a living fashion.

ultraviolet-light initiated polymerization based on trithiocarbonate iniferters (TTCs).³¹ Though this polymerization displayed living behavior when conducted in solution, the corresponding gel growth was not well controlled. This limitation was the direct result of the mechanism of UV-induced polymerization using TTCs, which involves photolysis of a TTC to generate a propagating carbon-centered radical and an unstable trithiocarbonate radical. In solution, these reactions

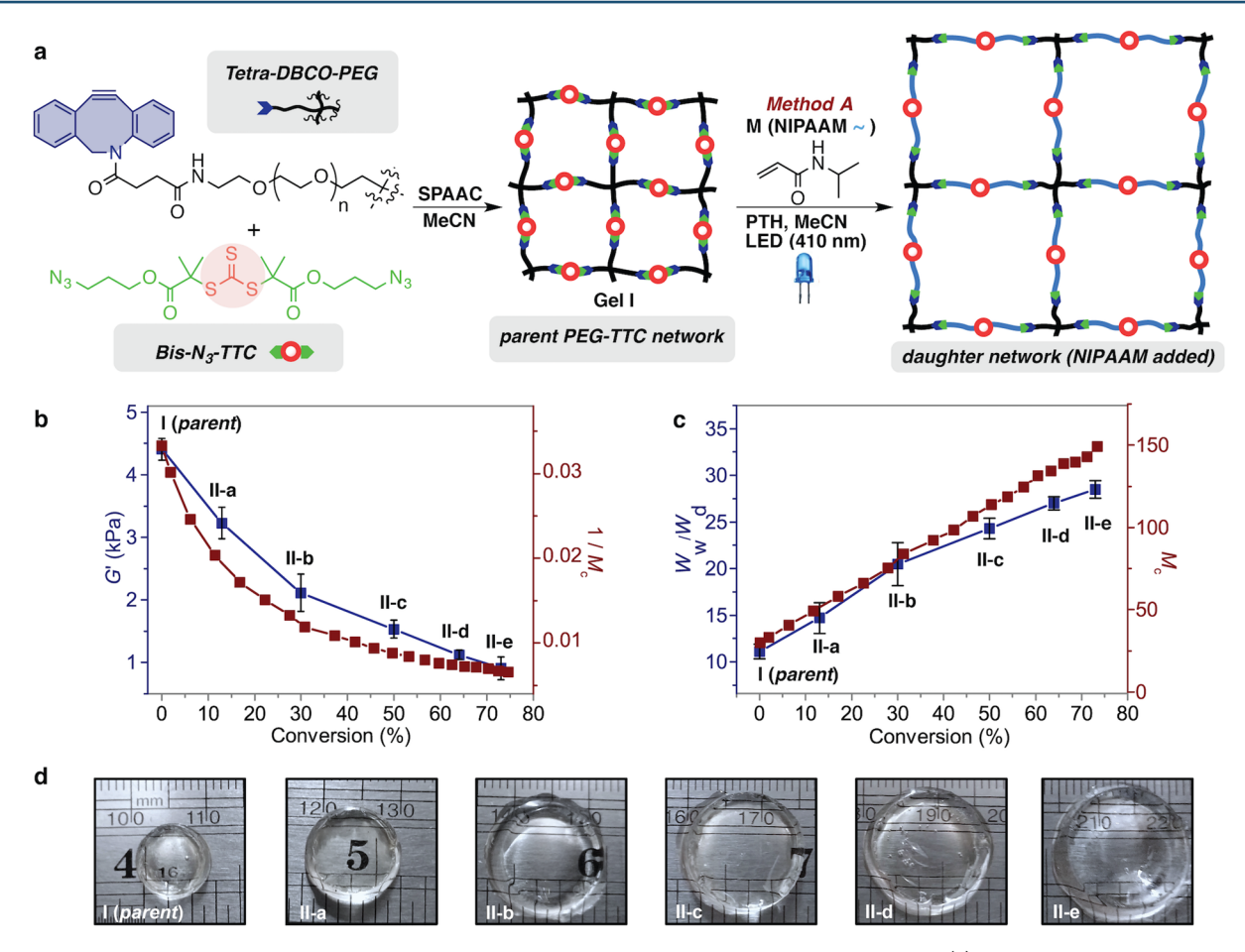


Figure 3. Living additive manufacturing via PRCG insertion of NIPAAM into a parent PEG-TTC network. (a) Parent network design. Gelation is achieved by SPAAC click chemistry. PRCG is conducted in the presence of monomer and PTH under blue LED irradiation. (b) Experimental storage modulus G' (blue curve) and simulated results of inverse of average chain length $(1/M_c)$ between junctions (red curve) as a function of monomer conversion in PRCG. (c) Swelling ratio (blue curve). Defined as W_w/W_d , where W_w is the weight of a sample swollen in pure water at 20 °C; W_d is the weight of this sample in the dry state) and simulated average chain length between network junctions, M_{cl} (red curve) as a function of monomer conversion. (d) Optical images of parent gel I and daughter gels II-a to II-e swollen in pure water at 20 °C.

display living behavior when a low light intensity is used, and when the concentration of TTC is high (~mM regime); this scenario ensures that the unstable TTC radical can be stabilized by another equivalent of nonphotolyzed TTC.³⁴ In our experience, when TTCs were embedded within polymer network strands, regions of the sample near the surface absorbed the most light and underwent uncontrolled polymerization/decomposition; it was impossible to achieve uniform, living chain growth throughout the entire network. In 2015, Kloxin and co-workers reported a similar study using UVactivation of dithiocarbamate iniferters embedded in polymer network strands.³² Here, dimethacrylate cross-linkers were inserted into the network strands under UV irradiation. No discussion of the livingness of this reaction was provided, but given the close mechanistic relationship to our previous work³¹ it is unlikely that the process was highly controllable at the molecular level.

Because the limitations of the above systems are the direct result of the UV-induced photolysis mechanism of polymerization, and the resulting unstable trithiocarbonate radical intermediates, we sought a living polymerization process capable of monomer insertion into polymer chains that would proceed via different reactive intermediates. Recently, inspired by developments in organic synthesis, 35 a plethora of photoredox catalyzed polymerization reactions have emerged.

These methods include variants of atom-transfer radical polymerization (ATRP),³⁶⁻⁴¹ reversible addition–fragmentation chain transfer (RAFT)/iniferter polymerization, 42-45 ringopening metathesis polymerization (ROMP),46 and cationic polymerization. ^{47,48} In 2015, inspired by the work of Boyer and co-workers, 42 we reported on the solution-phase photocontrolled radical polymerization of several acrylate and acrylamide monomers mediated by symmetric TTC iniferters and the photoredox catalyst 10-phenylphenothiazine (PTH).⁴³ We found that this polymerization greatly outperformed the traditional UV-induced direct TTC photolysis iniferter polymerization allowing the synthesis of polymers with higher molecular weights and greater control over molecular weight distributions. This increased control is thought to arise from differences in the reaction mechanisms: in the PTH-catalyzed process, photoinduced single electron transfer from PTH to the TTC induces the formation of a propagating radical, a TTC anion, and the PTH radical cation; the unstable TTC radical that leads to irreversible termination in the UV-photolysis method is not produced. Furthermore, because this photoredox polymerization involves excitation of a catalytic amount of PTH using visible light, it is possible to achieve uniform irradiation and living polymerization over larger reaction volumes. We reasoned that these features, made possible by the use of a distinct photoredox catalysis mechanism, could be harnessed to realize

our goal of living additive manufacturing as described in Figure 1b.

Herein, we report proof-of-concept studies of living additive manufacturing via photoredox catalyzed growth (PRCG) of uniform polymer gels (Figure 2a). PRCG begins with the synthesis of a homogeneous end-linked gel bearing TTC iniferters within the network strands. This "parent" gel is then exposed to a solution containing PTH photocatalyst, monomers (M), and cross-linkers (CL). Irradiation with blue LED light excites PTH in solution and initiates the living insertion of M and CL from solution into the network strands following the photoredox catalysis mechanism described in Figure 2b. This process avoids the formation of unstable TTC radicals; it enables the living insertion of new functionality into the strands of polymer networks (e.g., Figure 1b) to produce diverse daughter materials. We use PRCG to control network composition and mesh size, parameters that synergistically dictate the macroscopic properties of gels. 49-53 Thus, we are able to produce daughter gels with homogeneously altered compositions and either increased stiffness, decreased stiffness, or no net change in stiffness compared to the parent gel, all outcomes that could not be achieved using traditional free radical polymerization (Figure 1a). Furthermore, progeny gels with unique compositions, shapes, and patterned behaviors, such as temperature and polarity responsiveness, are fabricated by photowelding of daughter gels with different compositions. To validate the living nature of PRCG, we conducted gel disassembly experiments and simulations, showing that the macroscopic gel properties achieved experimentally (such as shear storage modulus (G') and swelling ratio (W_w/W_d) can be directly traced to PRCG-induced uniform increases in the molecular weight between network junctions.

■ RESULTS AND DISCUSSION

Living Insertion of NIPAAM into TTC-Containing Parent Polymer Networks via PRCG. We first investigated the feasibility of using photoredox catalyzed activation of TTCs for living polymer growth in solution and in parent gel networks bearing TTC groups. As expected, exposure of a solution of NIPAAM and a TTC iniferter to blue LED light (410 nm, 0.20 mW/cm²) in the presence of PTH catalyst led to highly controlled polymer growth (see Section C in Supporting Information for details of solution polymerization studies). The molecular weight of the polyNIPAAM product increased linearly with monomer conversion as monitored by gel permeation chromatography (GPC). When no PTH was added, the NIPAAM conversion remained below 5% after 24 h of irradiation.

Next, parent networks (gel I, Figure 3a) containing TTC groups embedded in each strand were formed via strain promoted alkyne—azide cycloaddition (SPAAC)^{54–56} coupling of a four-arm polyethylene glycol (PEG) star polymer terminated with dibenzocyclooctyne (Tetra-DBCO-PEG) and a bis-azide TTC (bis-N₃-TTC) (Figure 3a) in the presence of PTH and NIPAAM (0.75 mM and 2.5 M, respectively; see Methods section for details). Then, the parent gels were exposed to blue LED irradiation (method A, Figure 3a) to induce insertion of NIPAAM into the network strands following the mechanism outlined in Figure 2b. NIPAAM conversion was determined by proton nuclear magnetic resonance (¹H NMR) analysis of extracted sol fractions (see section D in Supporting Information for experimental operation). By varying the exposure time, five daughter gels

(II-a to II-e, Figure 3), each with a different NIPAAM composition (up to 73% NIPAAM conversion), were produced.

To assess the impact of PRCG on the daughter gel properties, G' values for water-swollen daughter hydrogels IIa to II-e and parent hydrogel I were measured using oscillatory rheometry. As shown in Figure 3b, G' gradually decreased from 4400 to 900 Pa as monomer conversion increased, which is expected given that insertion of NIPAAM leads to a decrease in cross-linking density (Figure 3a). Irradiation of the parent gel I in the absence of either NIPAAM or PTH or both afforded no change in G' (see Section D in Supporting Information). Simulation of the PRCG monomer insertion process using dissipative particle dynamics indicated that the chain length between network junctions (M_c) increased as the conversion increased (red curve, Figure 3b); the inverse of M_c followed a similar trend as the measured G' (see section F in Supporting Information for simulation).³³ The similarity between these two curves can be explained using rubber elasticity theory, which states that G' is proportional to the average chain length between junctions (neglecting topological defects). 57,58 Since daughter materials II-a to II-e differ from each other in terms of NIPAAM conversion, a more detailed treatment that takes into account the polymer volume fraction in the preparation state (ϕ_0) and in the swollen state (ϕ) is provided in Figure S16 (section G of Supporting Information). This corrected G' also shows very good agreement with the simulated results. To examine the effect of the newly incorporated monomers on the swelling behavior of gels in aqueous media, the swelling ratios (W_w/W_d) were measured for parent gel I and daughter gels II-a to II-e. As illustrated in Figure 3c, when the monomer conversion increased from $\bar{0}$ to 73%, the $W_{\rm w}/W_{\rm d}$ value increased approximately 3-fold (from 11 to 30); these data also tracked with the simulated M_c (red curve, Figure 3c), as swelling theory would predict.⁵⁷ Similarly, a more detailed treatment taking ϕ_0 and ϕ into account provided even better agreement between the experimental and simulated results (see Figure S17 in Section G of Supporting Information). Optical images of the parent and daughter gels (Figure 3d) show that increased monomer conversion leads to progressively larger daughter gels; PRCG enables macroscopic gel growth.

To verify that PRCG is a living process, we conducted gel disassembly studies to analyze the molecular weight and dispersity of the parent and daughter network strands. The experimental design for this procedure is outlined in Figure 4a. Aminolysis of the TTC groups in the parent gel I via exposure to excess piperidine yields soluble 11.3 kDa star polymers, as expected given the mass of Tetra-DBCO-PEG (Figure 4b). Analogous aminolysis of four daughter gels prepared via PRCG for 1-4 h also yielded star polymer products; these products reflected the original mass of the Tetra-DBCO-PEG plus the newly grown polyNIPAAM (Figure 4b). Consistent with a living process, the molar masses of these disassembly products progressively increased with irradiation time; the dispersity indices stayed relatively low (≤ 1.35), and there was no significant low molecular weight tailing. A high molecular weight shoulder was observed in each case, including for the parent gel (labeled with * in Figure 4b), which we attribute to disulfide bond formation between the thiol-terminated star polymer disassembly products. Nevertheless, these data represent an enormous improvement over the poorly controlled UV-induced process we reported previously;³¹

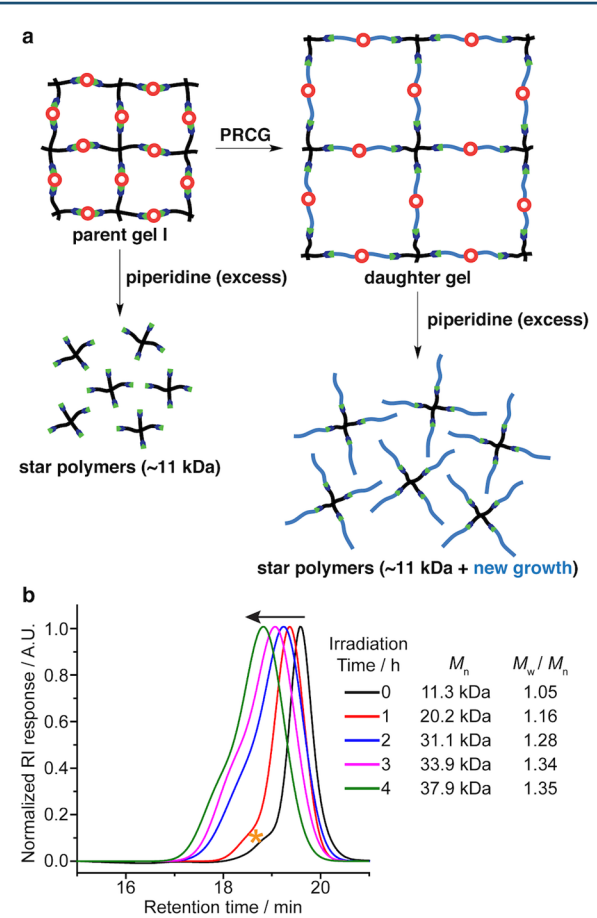


Figure 4. Network disassembly studies to verify the controlled nature of PRCG. (a) Aminolysis of parent gel I and PRCG-produced daughter gels yields star polymer products. Strand growth in the daughter gels is reflected in the mass of the star polymer disassembly products. (b) GPC traces for parent (black) and daughter gels prepared after PRCG for 1–4 h. Note: aminolysis produces star polymers with thiol chain ends. Due to a small amount of disulfide bond formation between these products, a high molecular weight shoulder is typically observed (labeled with * on the parent gel GPC trace) in these samples.

these are, to our knowledge, the first examples of living additive manufacturing via a photocontrolled process.

Living Insertion of Various Monomers and Cross-linkers into TTC-Containing Parent Polymer Networks via PRCG. Having demonstrated that PRCG can facilitate living additive manufacturing of daughter gels via controlled insertion of NIPAAM we sought to further control the daughter network structure and properties by combined addition of monomers and cross-linkers. In the studies described above (Figure 3), network growth occurred concomitantly with a softening of the material. We envisioned that through the use of mixtures of M and CL, chain extension could be offset by the introduction of new cross-links to enable decoupling of the network composition from mechanics (Figure 5a). In this approach, daughter gels with novel compositions and precise cross-linking densities, and therefore tunable mechanical properties, could be produced from the same parent gel.

To demonstrate this concept, PRCG was used to prepare a series of daughter gels (III-a to III-f) from the parent gel I via insertion of bis-acrylamide cross-linker and NIPAAM in various ratios (method B, see Section E in Supporting Information; note: vinyl conversion was held constant at 70% for each

daughter sample as measured by ¹H NMR). G' values were measured for each daughter hydrogel. As shown in Figure 5b, when the molar ratio of cross-linker to monomer increased from 0.1% to 5.0%, G' varied from 1400 to 23100 Pa, respectively. Keeping in mind that parent gel I has a modulus of 4400 Pa (Figure 3b), these data show that it is possible to produce softer or stiffer daughter gels, each with the same NIPAAM content, by simply modulating the monomer to crosslinker ratio. The water swelling ratios (W_w/W_d) of gels from III-a to III-f were measured. As shown in Figure 5c (blue curve), a higher molar ratio of cross-linker/monomer led to a lower $W_{\rm w}/W_{\rm d}$ value, indicating a smaller mesh size for the corresponding daughter gel. According to simulation results (Figure 5c, red curve), the molar ratio of cross-linker/monomer indeed has a profound effect on the average M_c , which follows the same trend as the experimental $W_{\rm w}/W_{\rm d}$ values.⁵⁹ Since $M_{\rm c}$ and $W_{\rm w}/W_{\rm d}$ both describe the mesh size of polymer networks (see Figure S17 for a more detailed treatment), the consistency of the simulation and experimental results suggests that the PRCG process follows the kinetics of living polymerization. Optical images (Figure 5d) show the size of the swollen daughter hydrogels (III-a to III-f) as a function of the amount of cross-linker added. Here again, each material has the same overall monomer composition, but differences in cross-linking density lead to dramatically different swelling ratios.

Notably, among the six daughter gel samples prepared, III-c (cross-linker/monomer ratio = 0.5%) had the same G' and swelling ratio, within error, as the parent gel I. In other words, compared to gel I, III-c has a larger volume (it has grown in size) and a new composition but roughly the same mesh size and mechanical properties. The case of III-c highlights a key advantage of living PRCG: though there are many examples of generating softer or stiffer gels using light, to our knowledge, no other methods could accomplish this outcome of uniform network growth with no change in modulus. Practical implementation of PRCG will benefit from this ability to grow new materials without compromising their mechanical properties.

As for all of the samples in Figure 5b-d, daughter gel III-c was formed at 70% vinyl conversion. Simulations (Figure 5e and Figure S15) suggested that the monomers and cross-linkers are evenly distributed throughout the daughter network following PRCG. On the basis of these results, we speculated that the storage modulus could be similarly held constant between parent and daughter gels if the same cross-linker/ monomer ratio was used as for III-c (0.5%) but at different vinyl conversion values. To test this concept, three new daughter gels (IV-a to IV-c) were produced with 0.5% crosslinker/monomer at different values of vinyl conversion (see section E-5 in Supporting Information for details). As shown in Figure 5f, G' and W_w/W_d values for these materials were similar to those of gel I. Thus, though these materials have different compositions their mechanical properties are very similar. The 0.5% cross-linker/monomer ratio appears in this case to be generally applicable for achieving uniform daughter gel growth with minimal impact on mechanics.

Having demonstrated living additive manufacturing via PRCG with NIPAAM monomer and cross-linkers, we next studied the monomer scope of this system by replacement of NIPAAM with other monomers. A series of daughter gels with varying cross-linker/monomer ratios were first prepared where NIPAAM was replaced with the hydrophobic monomer *n*-butyl acrylate (BA). In contrast to the NIPAAM materials described

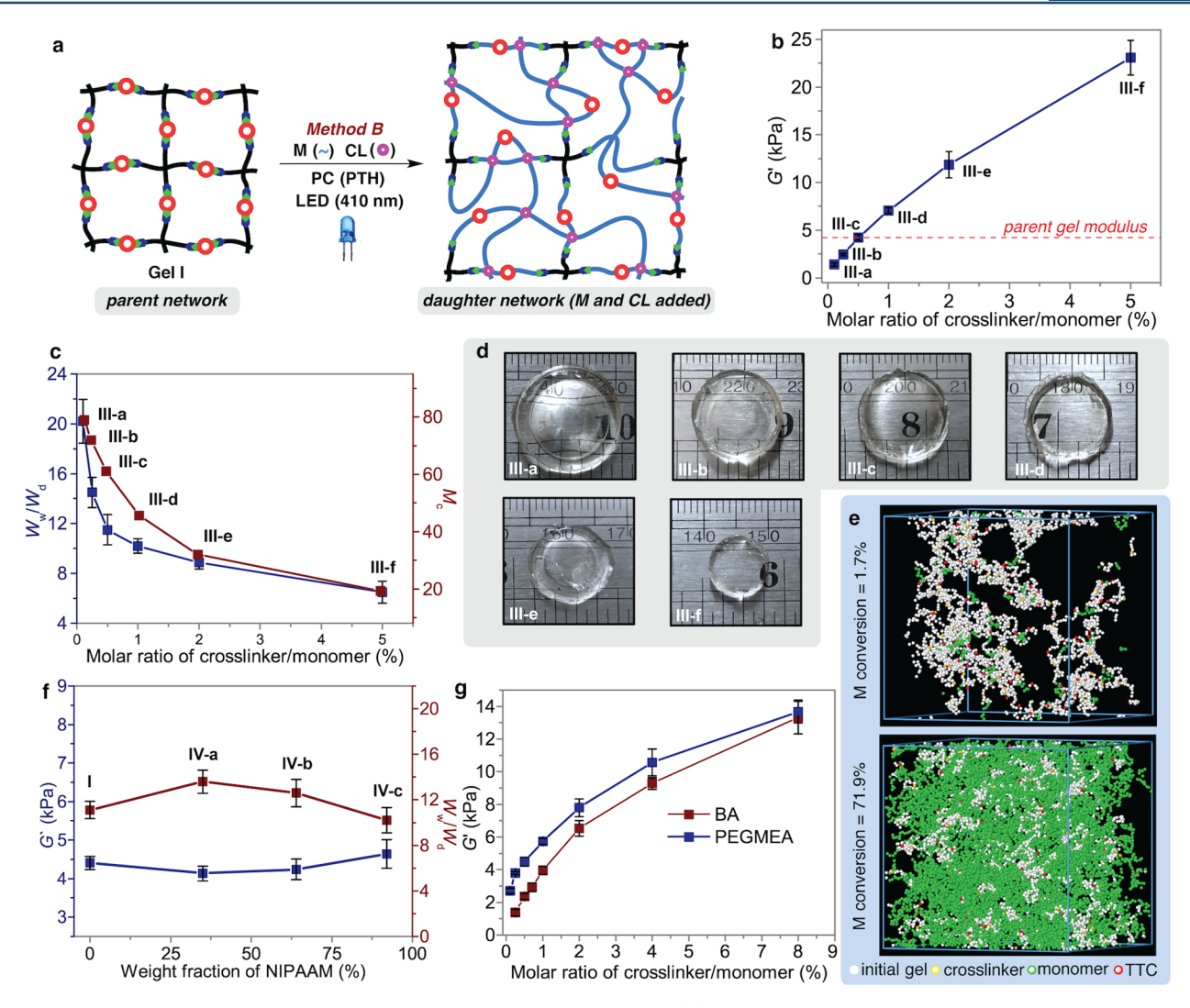


Figure 5. Living additive manufacturing via PRCG with monomers and cross-linker. (a) Schematic for PRCG in the presence of monomer and cross-linker. (b) The storage modulus of gel samples as a function of the cross-linker/monomer ratio. (c) Weight ratios of gel samples (blue curve) swollen in pure $H_2O(W_w)$ and at dry state (W_d) , and simulated average chain length between network junctions (red curve) as a function of the cross-linker/monomer molar ratio. (d) Optical images of gel samples (III-a to III-f) swollen in pure water. (e) Images showing the simulated networks before (top) and after (bottom) PRCG in the presence of monomer and cross-linker (unreacted beads are not shown for visual clarity). (f) The storage moduli (blue curve) and weight ratios of gel samples (red curve) swollen in pure $H_2O(W_w)$ and in the dry state (W_d) as a function of the PNIPAAM weight fraction in dry gels. (g) The effect of the cross-linker/monomer molar ratio on the storage moduli of gels produced using two different monomers. Red curve: M = BA, CL = neopentyl glycol diacrylate, swollen in DMF at 20 °C; Blue curve: M = PEGMEA, CL = neopentyl glycol diacrylate, swollen in pure water at 20 °C.

above, these BA-modified daughter gels collapsed in water but swelled in DMF, reflecting the difference in polarity of BA compared to NIPAAM. The G' values for DMF-swollen BAgels ranged from 1400 to 13300 Pa depending on the amount of CL used (Figure 5g). Similarly, hydrophilic poly(ethylene glycol) methyl ether acrylate (PEGMEA) monomer was used in place of NIPAAM, which resulted in water-swellable daughter hydrogels with G' values varying between 2700 and 13700 Pa depending on the amount of CL used (Figure 5g). For both BA and PEGMEA monomers, by using the correct cross-linker/monomer ratio and varying the irradiation time (i.e., vinyl conversion), it was possible to fabricate a series of daughter gels that differed in size and composition but had the same G' as the parent gel I. Collectively, these results demonstrate that PRCG is a general strategy to achieve living additive manufacturing of daughter gels with a range of mechanical strengths and chemical compositions where these

two factors are decoupled via the use of cross-linker and monomer mixtures.

Living Additive Manufacturing of Stimuli-Responsive "Smart" Materials via PRCG. Next, we investigated the use of living additive manufacturing via PRCG to generate daughter gels with stimuli responsive properties that were not present in the parent gel. The lower critical solution temperature (LCST) behavior of polyNIPAAM in water is well-known; ⁶⁰ we reasoned that daughter gels produced via insertion of different amounts of NIPAAM should display varied LCST behaviors compared to the parent PEG gel I. To demonstrate this concept, we first measured the temperature dependence of the storage moduli of gel I and NIPAAM-inserted daughter gels IV-a to IV-c. As shown in Figure 6a, while the G' value of the parent network I did not change significantly in the temperature range from 20 to 50 °C, the storage moduli of daughter gels IV-a to IV-c, with increasing mass fractions of

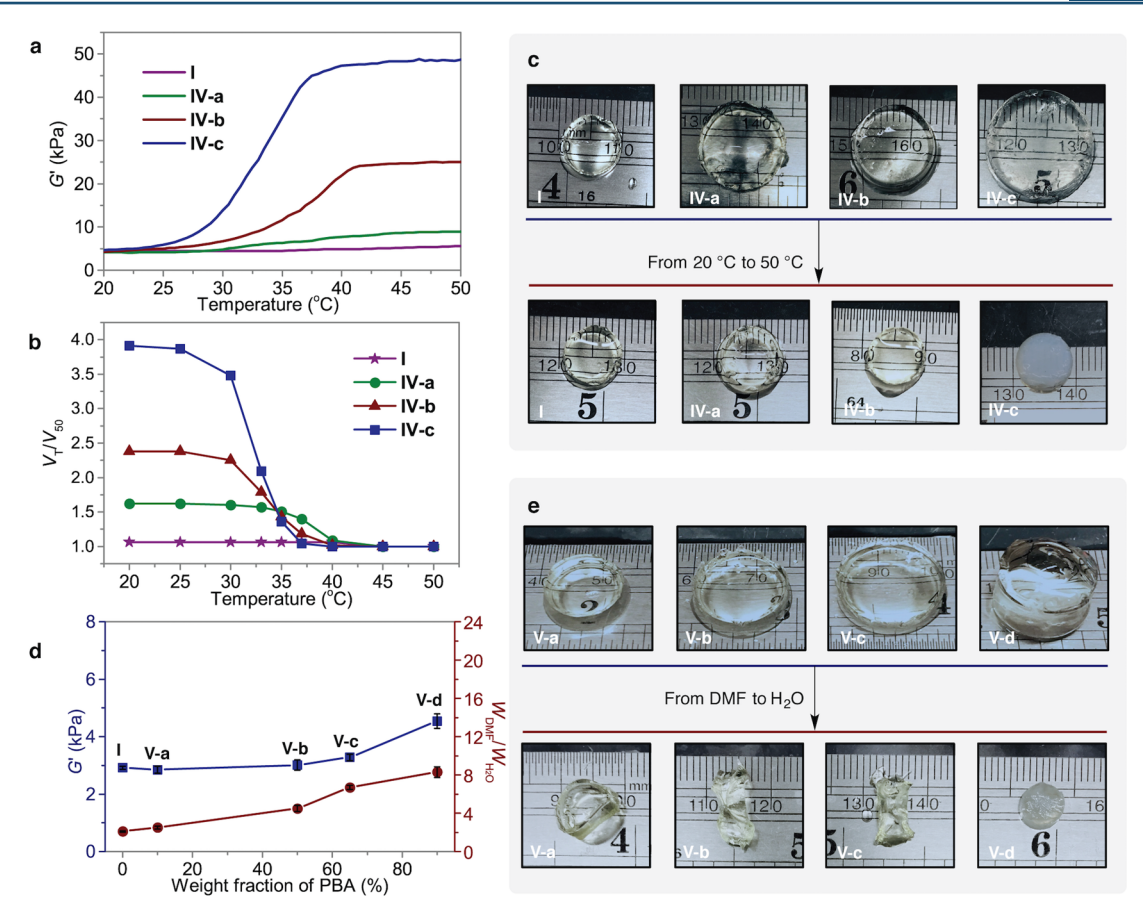


Figure 6. Daughter gels with variable properties by PRCG insertion of new monomers into the parent gel I. (a and b) For daughter samples IV-a to IV-c, mass fractions of NIPAAM are increasing, see Figure 5F. (a) Temperature dependence of the storage modulus of parent gel I and daughter gels IV-a to IV-c. (b) Temperature dependence of the equilibrium swelling volume ratios of parent gel I and daughter gels IV-a to IV-c, in which $V_{\rm T}$ and $V_{\rm S0}$ are the equilibrium volumes of hydrogels at T and 50 °C, respectively. (c) Optical images of the hydrogel samples I and IV-a to IV-c in the swollen state at 20 °C (<LCST) and in the collapsed state at 50 °C (>LCST) in pure water. (d) Storage moduli (blue curve) for daughter gels V-a to V-d (swollen in DMF) and their weight ratios (red curve) in DMF and water as a function of the weight fraction of PBA in dry gels. (e) Optical images of daughter gel samples V-a to V-d swollen in DMF and collapsed in pure water, both at 20 °C.

PNIPAAM, began to increase at ~25 °C and plateaued at higher temperatures to final values that were 2.1, 6.0, and 9.1 times, respectively, their initial values at 20 °C. These data indicate that the degree of increase in G' above LCST is closely related to the mass fraction of NIPAAM in the materials, a wellknown phenomenon in other NIPAAM copolymer materials. 61-64 We also investigated the temperature dependence of the equilibrium swelling ratios of these samples (Figure 6b). When the temperature was gradually raised above the LCST, the changes in the swelling ratios became increasingly greater $(V_{20}/V_{50} = 1.6, 2.4, \text{ and } 3.9, \text{ respectively})$ as the mass fraction of NIPAAM increased from IV-a to IV-c. Optical images provided in Figure 6c clearly show the volume changes of the daughter gels upon changing the temperature from 20 to 50 °C. Sample IV-c, which has the most NIPAAM, not only shows a large volume change, but also a shift from transparent to opaque. These transformations are fully reversible, which suggests that living additive manufacturing via PRCG could offer a versatile strategy for the fabrication of complex thermally responsive mechanical or optical gel actuators.

Next, we envisioned that by tuning the conversion of BA within daughter gels a series of hydrophobic gels with the same storage moduli in organic solvent (DMF), but different swelling behaviors in water, could be prepared from the parent gel I. Samples V-a to V-c, which contained increased mass fractions

of PBA (10%, 49%, and 65%, respectively), were prepared from gel I using a mixture of BA and 0.7 mol % CL. G' values for this series of gels swollen in DMF were fairly consistent (Figure 6d, blue curve), indicating that if the proper ratio of CL/monomer is chosen, the stiffness of the daughter gels can be maintained during the course of PRCG. However, as also shown in Figure 6d (red curve), the weight ratios (W_{DMF}/W_{H2O}) of these samples when swollen in DMF or water at 20 °C gradually increased from 2.1 to 6.7 as the percentage of BA increased. In particular, when 90% BA was incorporated (sample V-d see and Section E-6 in Supporting Information), a weight ratio $(W_{DMF}/$ $W_{\rm H2O}$) as high as 8.3 was observed. These differences in daughter gel volume in DMF versus water can be seen in the optical images provided in Figure 6e; when daughter gel V-d was moved from DMF to water, it not only underwent a significant size change (Figure 6e, bottom right), but also experienced a transparent-to-opaque transition as a result of the high mass fraction of hydrophobic BA. To summarize, the incorporation of hydrophobic BA monomer into parent gel I produces daughter gels with completely changed solubility properties and yet a constant stiffness in organic solvents, a feat that would be impossible using existing nonliving polymerization techniques.

Healing and Welding Daughter Gels with PRCG. Having demonstrated that PRCG provides a straightforward

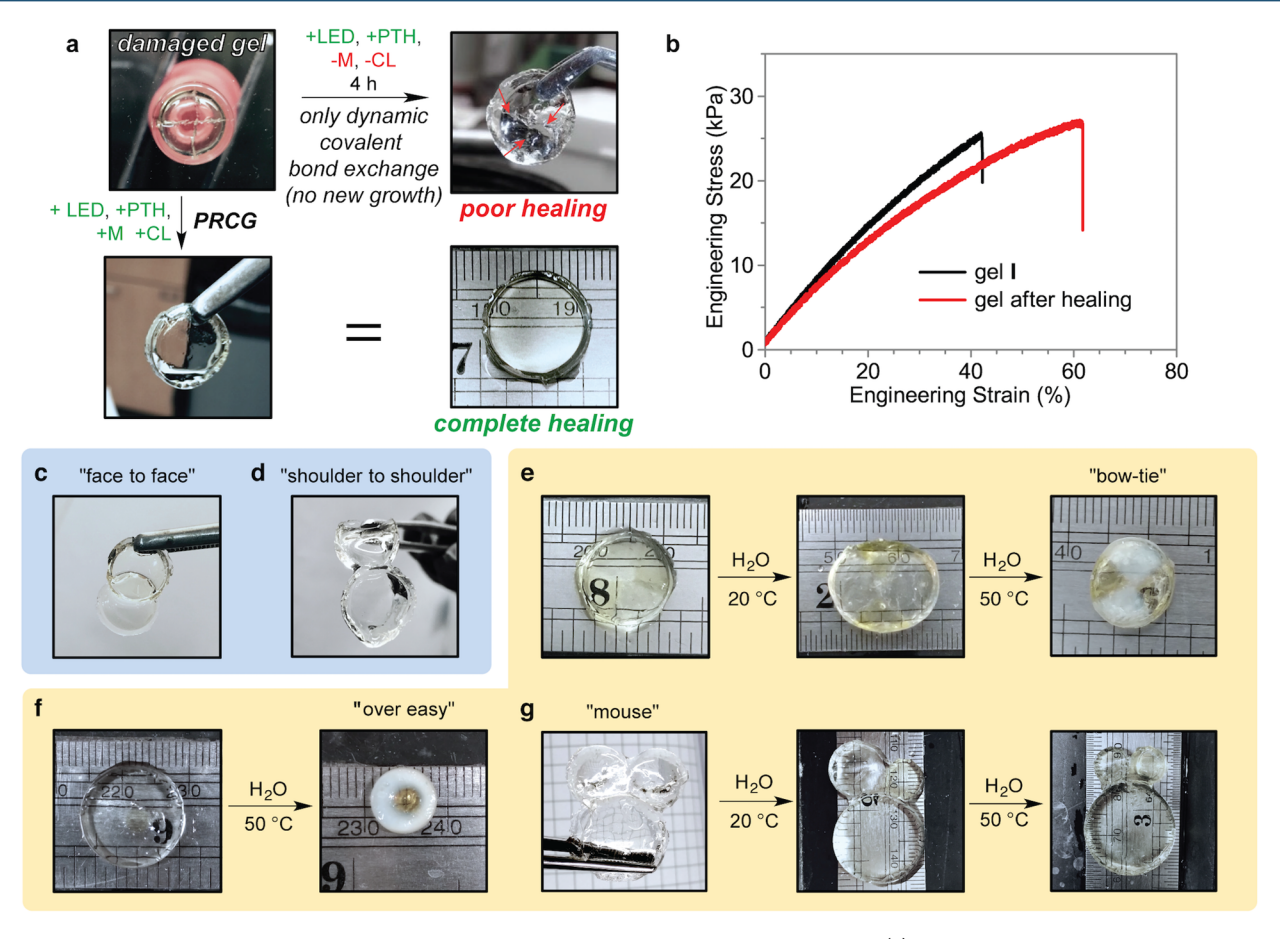


Figure 7. Applying PRCG as a versatile tool for gel healing, welding, and smart material fabrication. (a) Optical images of damaged hydrogel I after exposure to blue LED light in the absence and presence of monomer, cross-linker, and PTH. (b) Tensile response stress—strain curves for gel I and a gel sample after VLPH-induced healing. (c and d) Optical images illustrating photogrowth induced welding of two separated gels. (e–g) Optical images showing smart materials with site-specific stimuli-responsiveness properties produced by VLPG. (e) Appearance change from a disk-shaped gel to a "bow-tie" like gel. (f) Appearance change from a disk-shaped gel to an "over easy" like gel. (g) Appearance changes of a "mouse" like gel.

approach to simultaneously regulate the mechanical properties and chemical compositions of gels, we sought to investigate further its potential in a range of gel fabrication and modification applications. Given that these networks are built from dynamic covalent TTC groups, we expected that they should be able to undergo photoinduced healing when damaged.^{26,30} First, we examined the healing behavior of the parent PEG-TTC gel I under blue LED light in the presence of PTH but absence of monomer or cross-linker. As shown in Figure 7a, when a severely cut sample (gel I was cut in a cross direction) was directly irradiated with blue LED light for 4 h, the resulting gel still had visible nicks where it was cut; healing in the absence of additional monomer or cross-linker was not effective in this system. In contrast, if the damaged gel was first treated with a solution containing NIPAAM, bis-acrylamide, and PTH, and then exposed to blue LED light for 4 h, a healed gel with no visible damage was obtained. Tensile testing experiments (Figure 7b) revealed that the tensile modulus and toughness of the healed material were not decreased relative to those of the precut parent gel I. In the low strain region, the stress-strain curves for gel I and the healed sample had similar slopes; the precut and healed materials had similar tensile moduli. The healed gel displayed enhanced toughness (from 6 $\pm 1 \text{ J·m}^3$ to $13 \pm 3 \text{ J·m}^3$; see Supporting Information Section H), which could be ascribed to the introduction of new crosslinks at the severed interface during the PRCG healing process.

Given that it is possible to heal severed gels via PRCG, it should also be possible to weld together independently synthesized parent and/or daughter gels to produce new complex gel progeny with distinct spatially differentiated compositions. To demonstrate this welding process, we prepared two identical parent gel I samples, each containing monomer, cross-linker, and PTH. These parent gels were then placed in direct contact in either a "face to face" or "shoulder to shoulder" orientation and exposed to blue LED light. As shown in Figure 7c and Figure 7d, PRCG led to a robust fusion of the two parent gels; the welded gels could be repeatedly bent to up to 90° without fracture.

Finally, sincePRCG offers a convenient strategy for modifying the composition and mechanics of gels, and the capability of controlling polymerization both spatially and temporally using light, we reasoned that it should be possible to use this method to fabricate spatially responsive materials. To demonstrate this concept, three new progeny gels (Figure 7e,g) were prepared from the same parent gel I using a series of PRCG processes (see section H-3 in Supporting Information for details); here again, such a feat would be impossible without the living nature of PRCG, which enables repeatable reactivation of the network strands multiple times to achieve successive growth and welding events. In Figure 7e, two NIPAAM-containing daughter gels were welded together with two PBA-containing daughter gels. When this complex progeny

gel was swollen in organic solvents (i.e., MeCN), where all domains are swollen, a disk-shaped gel material was afforded (Figure 7e, far left). Immersing the material in water at 20 °C led to collapse of the PBA components, resulting in an ovalshaped gel (Figure 7e, center). When the water temperature was raised to 50 °C (above the LCST of polyNIPAAM), the polyNIPAAM components of the material collapsed and become opaque (Figure 7e, right), producing a "bow-tie" like appearance. In another example (Figure 7f), a ring-shaped daughter gel and a round daughter gel, each containing different mass fractions of NIPAAM, were prepared separately via PRCG and then welded together via PRCG to produce a complex progeny material with varied NIPAAM content. This material appeared uniform when swollen in water at 20 °C; raising the temperature above LCST led to an "over easy egg" appearance due to the transparent-to-opaque transition in the outer ring, which contained a higher NIPAAM mass fraction. In the last example (Figure 7g), a "mouse" like progeny gel was prepared by PRCG welding together three different daughter gels each prepared by PRCG: one with a PEGMEA ("face"), one with NIPAAM ("left ear"), and one with BA ("right ear"). In organic solvent (MeCN), the "mouse" gel had symmetric features. In contrast, its "right ear" shrank upon exposure to water, while its "left ear" shrank upon heating above the LCST of polyNIPAAM. To our knowledge, these are the first examples of multistep living additive manufacturing to produce complex spatially patterned gel materials.

CONCLUSION

To conclude, we have developed a first-generation living additive manufacturing process called PRCG that enables the controlled insertion of monomers and cross-linkers into polymer networks to produce complex daughter objects from a single type of parent object. PRCG makes use of a newly developed photoredox catalyzed polymerization that avoids the undesired chain termination processes that are present in traditional free radical and iniferter polymerizations. Our approach enabled the fabrication of daughter gels with complex compositions and mechanical properties that would be difficult or impossible to achieve using traditional free radical polymerization methods. In particular, we demonstrated that with the proper cross-linker to monomer ratio, we could grow daughter gels to different dimensions with new network compositions and yet with unmodified mechanical properties; material composition and mechanics were decoupled. Excellent agreements between experimental and simulated PRCG results provided a firm rationale for the observed changes in gel properties that is based on the living increase of M_c and uniform changes in cross-linking density. It should be noted that this proof-of-concept work only hints at the potential of living additive manufacturing via PRCG as a tool for the synthesis of complex materials. For practical applications, PRCG will require extensive development: the polymerization rate should be increased by at least an order of magnitude, the oxygen tolerance should be thoroughly investigated, 42 and the expansion to bulk polymeric materials should be pursued; these studies are ongoing in our laboratory. Furthermore, one could imagine using traditional additive manufacturing devices to produce TTC-based networks suitable for subsequent living additive manufacturing modifications; the two approaches could work in concert to enable unprecedented material functions. We believe that these results represent an important first step in the development of living additive manufacturing.

METHODS

See Supporting Information for full descriptions of all methods, characterization data, experiments, and simulations.

Synthesis of Parent Gel I and Representative Living Additive Manufacturing via PRCG Experiment. An ovendried vial (1.8 mL) was charged with a solution (50 μ L) of tetra-DBCO-PEG (15.0 mM), monomer, PTH (0.03 mol % of monomer) without cross-linker (method A) and with crosslinker (method B) in acetonitrile (MeCN) in a glovebox. A solution (50 μL) of bis-N₃-TTC (30.0 mM) in MeCN was added in one portion into the vessel. The solution was vortexed to afford sufficient mixing. Gelation was observed within 10 min. The reaction was kept in the dark for 24 h to ensure maximal conversion. Then, the vessel was taken out from the glovebox and exposed to LED light irradiation in a cold room (4 °C) for the desired time. After the reaction, the gel was removed from the vessel and swollen in MeCN at room temperature. The MeCN solvent was exchanged for at least five times to completely extract unreacted NIPAAM from the gel. The collected organic solution was concentrated under a vacuum. Butyl benzoate was added into the mixture as an internal standard in the ¹H NMR experiment for the calculation of monomer conversion. MeCN was then removed to give a dry gel. The material was weighed to afford a dry weight (W_d) . Then, the dry gel was fully swollen in pure water at room temperature. The swollen weight (W_w) and modulus (G') were measured for this hydrogel. Swelling ratios were defined as the value of $W_{\rm w}/W_{\rm d}$. At least three gels were prepared and tested to obtain each data point.

ASSOCIATED CONTENT

S Supporting Information

The Supporting Information is available free of charge on the ACS Publications website at DOI: 10.1021/acscentsci.6b00335.

Synthetic methods (PDF)

AUTHOR INFORMATION

Corresponding Author

*E-mail: jaj2109@mit.edu.

ORCID ©

Mingjiang Zhong: 0000-0001-7533-4708 LaShanda T. J. Korley: 0000-0002-8266-5000 Jeremiah A. Johnson: 0000-0001-9157-6491

Present Addresses

¹(M.C.) State Key Laboratory of Molecular Engineering of Polymers, Department of Macromolecular Science, Fudan University, Shanghai 200433, China.

[¶](M.Z.) Department of Chemical and Environmental Engineering, Yale University, New Haven, CT 06511.

Author Contributions

M.C., Y.G., and J.A.J. conceived the key concepts. M.C., Y.G., and M. Z. conducted the synthesis and characterization experiments. M.C. and Y.G. analyzed the data. A.S., S.B., and A.C.B. conducted the simulation experiments. A.M.J. and L.T.K. conducted the tensile test experiment. M.C., Y. G., M.Z., and J.A.J. wrote the paper.

Author Contributions

[#]M.C. and Y.G. contributed equally.

Notes

The authors declare no competing financial interest.

ACKNOWLEDGMENTS

J.A.J. thanks the National Science Foundation (CHE-1334703) for support of this work. A.C.B. thanks the United States Department of Energy (DE-FG02-90ER45438) for the development of the simulations. L.T.J.K acknowledges support from the Defense University Research Instrumentation Program (DURIP) grant W911NF1110343.

REFERENCES

- (1) Yagci, Y.; Jockusch, S.; Turro, N. J. Photoinitiated Polymerization: Advances, Challenges, and Opportunities. *Macromolecules* **2010**, 43, 6245–6260.
- (2) Tumbleston, J. R.; Shirvanyants, D.; Ermoshkin, N.; Janusziewicz, R.; Johnson, A. R.; Kelly, D.; Chen, K.; Pinschmidt, R.; Rolland, J. P.; Ermoshkin, A.; et al. Continuous liquid interface production of 3D objects. *Science* **2015**, 347, 1349–1352.
- (3) Shatford, R.; Karanassios, V. 3D printing in chemistry: Past, present and future. *Proc. SPIE* **2016**, 9855 *Next-Generation Spectroscopic Technologies IX*, 98550B.
- (4) Lutz, J. F.; Lehn, J. M.; Meijer, E. W.; Matyjaszewski, K. From precision polymers to complex materials and systems. *Nat. Rev. Mater.* **2016**, *1*, 16024.
- (5) Leibfarth, F. A.; Mattson, K. M.; Fors, B. P.; Collins, H. A.; Hawker, C. J. External Regulation of Controlled Polymerizations. *Angew. Chem., Int. Ed.* **2013**, *52*, 199–210.
- (6) Chen, M.; Zhong, M. J.; Johnson, J. A. Light-Controlled Radical Polymerization: Mechanisms, Methods, and Applications. *Chem. Rev.* **2016**, *116*, 10167–10211.
- (7) Trotta, J. T.; Fors, B. P. Organic Catalysts for Photocontrolled Polymerizations. *Synlett* **2016**, 27, 702–713.
- (8) Corrigan, N.; Shanmugam, S.; Xu, J. T.; Boyer, C. Photocatalysis in organic and polymer synthesis. *Chem. Soc. Rev.* **2016**, *45*, 6165–6212.
- (9) Dadashi-Silab, S.; Doran, S.; Yagci, Y. Photoinduced Electron Transfer Reactions for Macromolecular Syntheses. *Chem. Rev.* **2016**, *116*, 10212–10275.
- (10) Lendlein, A.; Jiang, H. Y.; Junger, O.; Langer, R. Light-induced shape-memory polymers. *Nature* **2005**, 434, 879–882.
- (11) Ikeda, T.; Mamiya, J.; Yu, Y. L. Photomechanics of liquid-crystalline elastomers and other polymers. *Angew. Chem., Int. Ed.* **2007**, 46, 506–528.
- (12) Johnson, J. A.; Finn, M. G.; Koberstein, J. T.; Turro, N. J. Synthesis of photocleavable linear macromonomers by ATRP and star macromonomers by a tandem ATRP-click reaction: Precursors to photodegradable model networks. *Macromolecules* **2007**, *40*, 3589–3598.
- (13) Luo, Y.; Shoichet, M. S. A photolabile hydrogel for guided three-dimensional cell growth and migration. *Nat. Mater.* **2004**, *3*, 249–253.
- (14) Kobatake, S.; Takami, S.; Muto, H.; Ishikawa, T.; Irie, M. Rapid and reversible shape changes of molecular crystals on photoirradiation. *Nature* **2007**, *446*, 778–781.
- (15) Kloxin, A. M.; Kasko, A. M.; Salinas, C. N.; Anseth, K. S. Photodegradable hydrogels for dynamic tuning of physical and chemical properties. *Science* **2009**, *324*, 59–63.
- (16) van Oosten, C. L.; Bastiaansen, C. W. M.; Broer, D. J. Printed artificial cilia from liquid-crystal network actuators modularly driven by light. *Nat. Mater.* **2009**, *8*, 677–682.
- (17) Burnworth, M.; Tang, L. M.; Kumpfer, J. R.; Duncan, A. J.; Beyer, F. L.; Fiore, G. L.; Rowan, S. J.; Weder, C. Optically healable supramolecular polymers. *Nature* **2011**, 472, 334–338.
- (18) Yamaguchi, H.; Kobayashi, Y.; Kobayashi, R.; Takashima, Y.; Hashidzume, A.; Harada, A. Photoswitchable gel assembly based on molecular recognition. *Nat. Commun.* **2012**, *3*, 603.
- (19) Iamsaard, S.; Asshoff, S. J.; Matt, B.; Kudernac, T.; Cornelissen, J. J. L. M.; Fletcher, S. P.; Katsonis, N. Conversion of light into macroscopic helical motion. *Nat. Chem.* **2014**, *6*, 229–235.

(20) DeForest, C. A.; Tirrell, D. A. A photoreversible protein-patterning approach for guiding stem cell fate in three-dimensional gels. *Nat. Mater.* **2015**, *14*, 523–531.

- (21) Zhang, L. D.; Liang, H. R.; Jacob, J.; Naumov, P. Photogated humidity-driven motility. *Nat. Commun.* **2015**, *6*, 7429.
- (22) Cramer, N. B.; Scott, J. P.; Bowman, C. N. Photopolymerizations of thiol-ene polymers without photoinitiators. *Macromolecules* **2002**, *35*, 5361–5365.
- (23) Kloxin, C. J.; Scott, T. F.; Adzima, B. J.; Bowman, C. N. Covalent Adaptable Networks (CANS): A Unique Paradigm in Cross-Linked Polymers. *Macromolecules* **2010**, *43*, 2643–2653.
- (24) Scott, T. F.; Schneider, A. D.; Cook, W. D.; Bowman, C. N. Photoinduced plasticity in cross-linked polymers. *Science* **2005**, *308*, 1615–1617.
- (25) Meng, Y.; Fenoli, C. R.; Aguirre-Soto, A.; Bowman, C. N.; Anthamatten, M. Photoinduced Diffusion Through Polymer Networks. *Adv. Mater.* **2014**, *26*, 6497–6502.
- (26) Amamoto, Y.; Kamada, J.; Otsuka, H.; Takahara, A.; Matyjaszewski, K. Repeatable Photoinduced Self-Healing of Covalently Cross-Linked Polymers through Reshuffling of Trithiocarbonate Units. *Angew. Chem., Int. Ed.* **2011**, *50*, 1660–1663.
- (27) Amamoto, Y.; Kikuchi, M.; Masunaga, H.; Ogawa, H.; Sasaki, S.; Otsuka, H.; Takahara, A. Mesh-size control and functionalization of reorganizable chemical gels by monomer insertion into their cross-linking points. *Polym. Chem.* **2011**, *2*, 957–962.
- (28) Wojtecki, R. J.; Meador, M. A.; Rowan, S. J. Using the dynamic bond to access macroscopically responsive structurally dynamic polymers. *Nat. Mater.* **2011**, *10*, 14–27.
- (29) Amamoto, Y.; Otsuka, H.; Takahara, A.; Matyjaszewski, K. Changes in network structure of chemical gels controlled by solvent quality through photoinduced radical reshuffling reactions of trithiocarbonate units. ACS Macro Lett. 2012, 1, 478–481.
- (30) Amamoto, Y.; Otsuka, H.; Takahara, A.; Matyjaszewski, K. Self-Healing of Covalently Cross-Linked Polymers by Reshuffling Thiuram Disulfide Moieties in Air under Visible Light. *Adv. Mater.* **2012**, *24*, 3975–3980.
- (31) Zhou, H. X.; Johnson, J. A. Photo-controlled Growth of Telechelic Polymers and End-linked Polymer Gels. *Angew. Chem., Int. Ed.* **2013**, 52, 2235–2238.
- (32) Gordon, M. B.; French, J. M.; Wagner, N. J.; Kloxin, C. J. Dynamic Bonds in Covalently Crosslinked Polymer Networks for Photoactivated Strengthening and Healing. *Adv. Mater. (Weinheim, Ger.)* **2015**, 27, 8007–8010.
- (33) Singh, A.; Kuksenok, O.; Johnson, J. A.; Balazs, A. C. Tailoring the structure of polymer networks with iniferter-mediated photogrowth. *Polym. Chem.* **2016**, *7*, 2955–2964.
- (34) Wang, H.; Li, Q.; Dai, J.; Du, F.; Zheng, H.; Bai, R. Real-Time and in Situ Investigation of "Living"/Controlled Photopolymerization in the Presence of a Trithiocarbonate. *Macromolecules* **2013**, *46*, 2576–2582.
- (35) Prier, C. K.; Rankic, D. A.; MacMillan, D. W. C. Visible Light Photoredox Catalysis with Transition Metal Complexes: Applications in Organic Synthesis. *Chem. Rev.* **2013**, *113*, 5322–5363.
- (36) Fors, B. P.; Hawker, C. J. Control of a Living Radical Polymerization of Methacrylates by Light. *Angew. Chem., Int. Ed.* **2012**, *51*, 8850–8853.
- (37) Treat, N. J.; Sprafke, H.; Kramer, J. W.; Clark, P. G.; Barton, B. E.; de Alaniz, J. R.; Fors, B. P.; Hawker, C. J. Metal-Free Atom Transfer Radical Polymerization. *J. Am. Chem. Soc.* **2014**, *136*, 16096—16101
- (38) Miyake, G. M.; Theriot, J. C. Perylene as an Organic Photocatalyst for the Radical Polymerization of Functionalized Vinyl Monomers through Oxidative Quenching with Alkyl Bromides and Visible Light. *Macromolecules* **2014**, *47*, 8255–8261.
- (39) Pan, X. C.; Lamson, M.; Yan, J. J.; Matyjaszewski, K. Photoinduced Metal-Free Atom Transfer Radical Polymerization of Acrylonitrile. *ACS Macro Lett.* **2015**, *4*, 192–196.

(40) Theriot, J. C.; Lim, C. H.; Yang, H.; Ryan, M. D.; Musgrave, C. B.; Miyake, G. M. Organocatalyzed atom transfer radical polymerization driven by visible light. *Science* **2016**, 352, 1082–1086.

- (41) Pearson, R. M.; Lim, C. H.; McCarthy, B. G.; Musgrave, C. B.; Miyake, G. M. Organocatalyzed Atom Transfer Radical Polymerization Using N-Aryl Phenoxazines as Photoredox Catalysts. *J. Am. Chem. Soc.* **2016**, *138*, 11399–11407.
- (42) Xu, J. T.; Jung, K.; Atme, A.; Shanmugam, S.; Boyer, C. A Robust and Versatile Photoinduced Living Polymerization of Conjugated and Unconjugated Monomers and Its Oxygen Tolerance. *J. Am. Chem. Soc.* **2014**, *136*, 5508–5519.
- (43) Chen, M.; MacLeod, M. J.; Johnson, J. A. Visible-Light-Controlled Living Radical Polymerization from a Trithiocarbonate Inferter Mediated by an Organic Photoredox Catalyst. *ACS Macro Lett.* **2015**, *4*, 566–569.
- (44) Xu, J. T.; Shanmugam, S.; Duong, H. T.; Boyer, C. Organo-photocatalysts for photoinduced electron transfer-reversible addition-fragmentation chain transfer (PET-RAFT) polymerization. *Polym. Chem.* **2015**. *6*. 5615–5624.
- (45) Xu, J. T.; Shanmugam, S.; Fu, C. K.; Aguey-Zinsou, K. F.; Boyer, C. Selective Photoactivation: From a Single Unit Monomer Insertion Reaction to Controlled Polymer Architectures. *J. Am. Chem. Soc.* **2016**, 138, 3094—3106.
- (46) Ogawa, K. A.; Goetz, A. E.; Boydston, A. J. Metal-Free Ring-Opening Metathesis Polymerization. *J. Am. Chem. Soc.* **2015**, *137*, 1400–1403.
- (47) Perkowski, A. J.; You, W.; Nicewicz, D. A. Visible Light Photoinitiated Metal-Free Living Cationic Polymerization of 4-Methoxystyrene. *J. Am. Chem. Soc.* **2015**, *137*, 7580–7583.
- (48) Kottisch, V.; Michaudel, Q.; Fors, B. P. Cationic Polymerization of Vinyl Ethers Controlled by Visible Light. *J. Am. Chem. Soc.* **2016**, 138, 15535–15538.
- (49) Lee, K. Y.; Mooney, D. J. Hydrogels for tissue engineering. *Chem. Rev.* **2001**, *101*, 1869–1879.
- (50) Peppas, N. A.; Hilt, J. Z.; Khademhosseini, A.; Langer, R. Hydrogels in biology and medicine: From molecular principles to bionanotechnology. *Adv. Mater.* **2006**, *18*, 1345–1360.
- (51) Bastide, J.; Leibler, L. Large-Scale Heterogeneities in Randomly Cross-Linked Networks. *Macromolecules* 1988, 21, 2647–2649.
- (52) Rubinstein, M.; Panyukov, S. Elasticity of polymer networks. *Macromolecules* **2002**, 35, 6670–6686.
- (53) Hild, G. Model networks based on 'endlinking' processes: synthesis, structure and properties. *Prog. Polym. Sci.* **1998**, 23, 1019—1149.
- (54) Jewett, J. C.; Bertozzi, C. R. Cu-free click cycloaddition reactions in chemical biology. *Chem. Soc. Rev.* **2010**, *39*, 1272–1279.
- (55) Johnson, J. A.; Baskin, J. M.; Bertozzi, C. R.; Koberstein, J. T.; Turro, N. J. Copper-free click chemistry for the in situ crosslinking of photodegradable star polymers. *Chem. Commun.* **2008**, 3064–3066.
- (56) DeForest, C. A.; Polizzotti, B. D.; Anseth, K. S. Sequential click reactions for synthesizing and patterning three-dimensional cell microenvironments. *Nat. Mater.* **2009**, *8*, 659–664.
- (57) Rubinstein, M.; Colby, R. H. *Polymer Physics*; Oxford University Press: Oxford, 2003.
- (58) Zhong, M.; Wang, R.; Kawamoto, K.; Olsen, B. D.; Johnson, J. A. Quantifying the impact of molecular defects on polymer network elasticity. *Science* **2016**, 353, 1264–1268.
- (59) Although gel I and sample III-c have similar properties according to experimental results, their simulated M_c values (30 vs 65.2) are different, which can be explained by taking ϕ_0 into account (see Section G in Supporting Information).
- (60) Schild, H. G. Poly (N-Isopropylacrylamide) Experiment, Theory and Application. *Prog. Polym. Sci.* **1992**, *17*, 163–249.
- (61) Kaneko, Y.; Sakai, K.; Kikuchi, A.; Yoshida, R.; Sakurai, Y.; Okano, T. Influence of Freely Mobile Grafted Chain-Length on Dynamic Properties of Comb-Type Grafted Poly(N-Isopropylacrylamide) Hydrogels. *Macromolecules* 1995, 28, 7717–7723.

(62) Okajima, T.; Harada, I.; Nishio, K.; Hirotsu, S. Kinetics of volume phase transition in poly(N-isopropylacrylamide) gels. *J. Chem. Phys.* **2002**, *116*, 9068–9077.

- (63) Haraguchi, K.; Li, H. J. Control of the coil-to-globule transition and ultrahigh mechanical properties of PNIPA in nanocomposite hydrogels. *Angew. Chem., Int. Ed.* **2005**, *44*, 6500–6504.
- (64) Xia, L. W.; Xie, R.; Ju, X. J.; Wang, W.; Chen, Q. M.; Chu, L. Y. Nano-structured smart hydrogels with rapid response and high elasticity. *Nat. Commun.* **2013**, *4*, 1–11.
- (65) Maeda, S.; Hara, Y.; Yoshida, R.; Hashimoto, S. Active Polymer Gel Actuators. *Int. J. Mol. Sci.* **2010**, *11*, 52–66.